Experimental observation of spin–split energy dispersion in high-mobility single-layer graphene/WSe_2 heterostructures Supplementary Materials

Priya Tiwari[1], Mohit Kumar Jat[1], Adithi Udupa[2], Deepa S. Narang[1], Kenji Watanabe[3], Takashi Taniguchi[4], Diptiman Sen[1,2], Aveek Bid[1*]

[1]*Department of Physics, Indian Institute of Science, Bangalore 560012, India*

[2]*Centre for High Energy Physics, Indian Institute of Science, Bangalore 560012, India*

[3] *Research Center for Functional Materials, National Institute for Materials Science, 1-1 Namiki, Tsukuba 305-0044, Japan*

[4] *International Center for Materials Nanoarchitectonics, National Institute for Materials Science, 1-1 Namiki, Tsukuba 305-0044, Japan*

E-mail: aveek@iisc.ac.in

Device Fabrication and characterization

We fabricated heterostructures of single-layer graphene (SLG) and trilayer WSe_2, encapsulated by single-crystalline hBN flakes of thickness ∼20-30 nm. The SLG, WSe_2, and hBN flakes were obtained by mechanical exfoliation on SiO_2/Si wafer using scotch tape from the corresponding bulk crystals. The thickness of the flakes was verified both from optical contrast under an optical microscope and Raman spectroscopy.

The Raman data for SLG and trilayer WSe_2 flake are shown in Figs. S1(a) and (b) respectively. For the graphene, the high intensity of the Lorentzian G' peak confirms it to be a single-layer.

The flakes were formed into a heterostructure using dry transfer technique[1] using a home-built transfer set-up consisting of high-precision XYZ-manipulators, the entire process being performed under an optical microscope. Briefly, the hBN was first picked up using a Polycarbonate (PC) film at 90^oC. This combination was then used to pick up the SLG followed by WSe_2 and hBN. The prepared stack was transferred on a clean Si/SiO_2 wafer at 180^oC and cleaned using chloroform to remove the PC, and this was followed by cleaning with acetone and isopropyl alcohol. The heterostructure was then annealed at 250°C for 3 hours.

Electron beam lithography was used to define the edge contacts. The edge contact[2] was made by reactive ion etching (where the mixture of CHF_3 and O_2 gas was used with flow rates of 40 sccm and 4 sscm, respectively, at a temperature of 25°C at the RF power of 60 W). The electrical contacts were finally created by depositing Cr/Au (5/60 nm) followed by lift-off in hot acetone and IPA. The purpose of choosing Cr/Au is that it forms a very high quality ohmic contact with gaphene,[2] but at the same time it does not form any contact with WSe_2 due to high Schottky barrier and large difference in work function.[3,4] Finally, the device was etched into a Hall bar geometry. An optical image of the final device is shown in the main text (inset of Fig. 1(b)).

To estimate the impurity density (n_0) and field-effect mobility (μ) of the device, the gate-voltage dependent resistance data were fitted by the equation

$$R = 2R_c + L/We\mu\sqrt{n_0^2 + (V_{bg} - V_d)^2 C^2/e^2}, \tag{1}$$

where R_c is the contact resistance, L and W are the channel length and width, respectively, C is the capacitance per unit area, and V_d is the value of the back-gate voltage at the Dirac

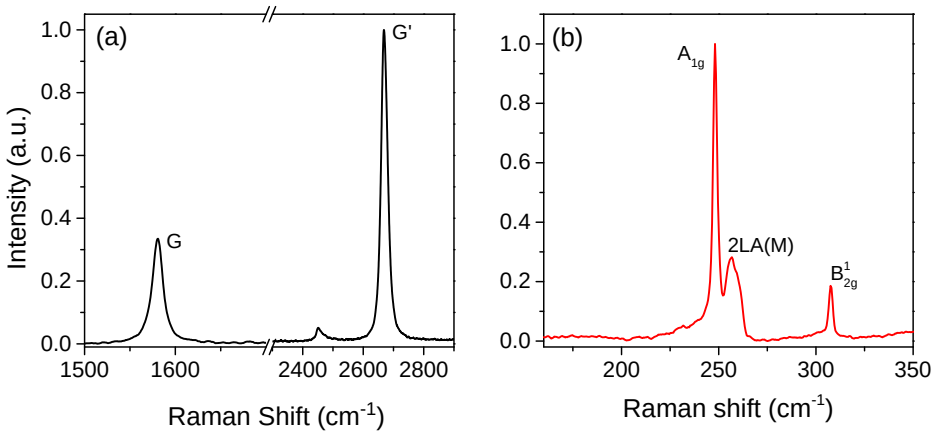

Figure S1: Room temperature Raman spectra for (a) the single-layer graphene and (b) the WSe_2 flake.

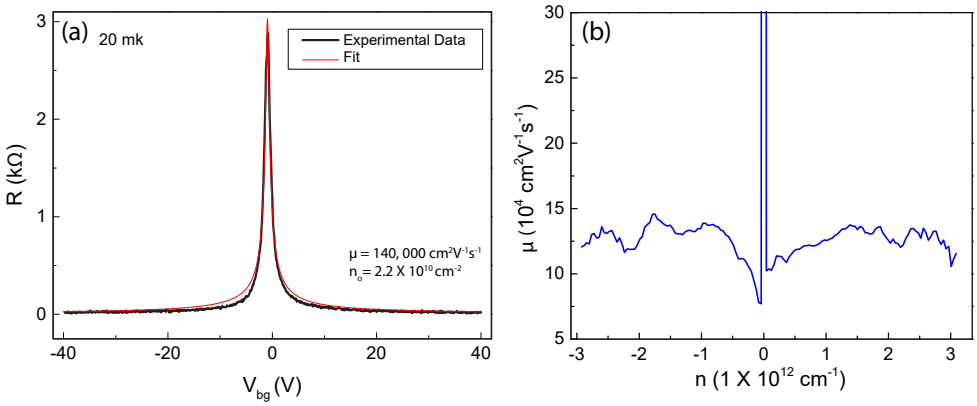

Figure S2: (a) Four probe resistance plotted as a function of gate voltage at 20 mK (shown by a black curve) - the red curve is the fit to the data for the extraction of mobility (μ) and impurity density (n_o). The μ of the device was $\sim 140,000$ cm^{2}V^{-1}s and the n_o was 2.2×10^{-14}m^{-2}. (b) Plot of mobility (μ) vs charge carrier density (n) at 20 mK.

point. Fig. S2(a) is the plot of four probe resistance versus gate voltage. The red curve is the fit using Eq. (1). The extracted n_o was $\sim 2.2 \times 10^{10}$ cm^{-2}, and μ was found to be nearly $\sim$140,000 cm^2 V^{-1}s^{-1}. Fig. S2(b) shows a plot of mobility versus charge carrier density (n), the data was plotted using the equation $\mu = \sigma/ne$, where $n = C(V_{bg} - V_d)/e$ and σ is conductivity. One can see that away from the Dirac point, the mobility is nearly independent of n.

Calculation of the dispersion relation

We extract the effective mass m^* by fitting the normalized amplitude of longitudinal resistivity to the relation:[5,6]

$$\frac{\Delta R_{xx}}{R_0} \propto \frac{2\pi^2 k_B T m^*/\hbar eB}{sinh\left(2\pi^2 k_B T m^*/\hbar eB\right)}, \tag{2}$$

where δR_{xx} is the amplitude of longitudinal resistivity and R_o longitudinal resistivity at zero magnetic fields.

The effective mass can be written as

$$\begin{aligned} m^{*-1} &= \frac{1}{\hbar^2}\frac{\partial^2 E}{\partial k^2}, \\ m^{*-1} &= \frac{1}{\hbar^2}\frac{\partial}{\partial k}\left(\frac{\partial E}{\partial A_k}\times\frac{\partial A_k}{\partial k}\right). \end{aligned} \tag{3}$$

Using $A_k = \pi k^2$, $2\pi k dk = \partial A_k$ yields

$$\begin{aligned} m^{*-1} &= \frac{2\pi}{\hbar^2}\frac{\partial E}{\partial A_k}, \\ m^{*} &= \frac{\hbar^2}{2\pi}\frac{\partial A_k}{\partial E}. \end{aligned} \tag{4}$$

For $A_k = \pi k^2$ and for a linear dispersion of single layer graphene ($E = \hbar v_F k$), we have

$$\begin{aligned} A_k &= \pi\left(\frac{E}{\hbar v_F}\right)^2, \\ m^* &= \frac{E}{v_F^2} = \hbar\frac{k}{v_F}, \\ m^* &= \hbar\frac{\sqrt{\pi n}}{v_F} = \frac{\sqrt{\pi}\,\hbar}{v_F}\sqrt{n}. \end{aligned} \tag{5}$$

One can fit the experimentally obtained dependence of m^* on n using the relation $m^* = \sqrt{\pi}\hbar n^{\alpha}/v_F$[7] keeping α and v_F as fitting parameters. The fits to the experimental data shown in main text (see Fig.3(c)) yield $\alpha = 0.5 \pm 0.02$ and $v_F = 1.29 \pm 0.04 \times 10^6$ ms^{-1}. The value of α is nearly 0.5, establishing the dispersion relation between energy and momentum

for SLG/WSe_2 to be linear.[8]

Theoretical Modelling

The continuum Hamiltonian near the Dirac points used for fitting the experimental data has the following terms:

$$\begin{aligned} H &= \hbar v_F(\eta k_x\sigma_x + k_y\sigma_y) + \Delta\sigma_z + \lambda_{KM}\eta S_z\sigma_z + \lambda_{VZ}\eta S_z + \lambda_R(\eta S_y\sigma_x - S_x\sigma_y) \\ &\quad + \frac{\sqrt{3}a}{2}[\lambda^A_{PIA}(\sigma_z + \sigma_0) + \lambda^B_{PIA}(\sigma_z - \sigma_0)](k_xS_y - k_yS_x) \end{aligned} \tag{6}$$

The best fit gives hopping parameter $t = 3979.10 \pm 3.99$ meV implying a large Fermi velocity $v_F = 3ta/2$ in this sample. We further note that the parameters in the Hamiltonian which give the spin-split band gap in both conduction and valence bands are λ_{VZ} and λ_R. The other parameters do not significantly alter the dispersion in the region of experimental data.

We also find that the best fit gives the values of λ_{VZ} and λ_R to lie on a circle of radius 2.51 meV giving a spin-split band gap of $5meV$, such that

$$\lambda_{VZ} = 2.51\ \cos\theta\ \text{meV}, \lambda_{\text{R}} = 2.51\ \sin\theta\ \text{meV}, \tag{7}$$

The two extreme cases are given by $\theta = 0$ with only valley-Zeeman SOC and $\theta = \pi/2$ with only Rashba SOC are shown in Fig. S3. In absence of experimental data to fix θ, we take the value of λ_R from literature and produce a plot for $\lambda_R = 0.56\ meV$ and $\lambda_{VZ} = 2.45\ meV$ as shown in Fig. S3 (c). The actual dispersion of this sample will have a form very similar to Fig. S3 (c).

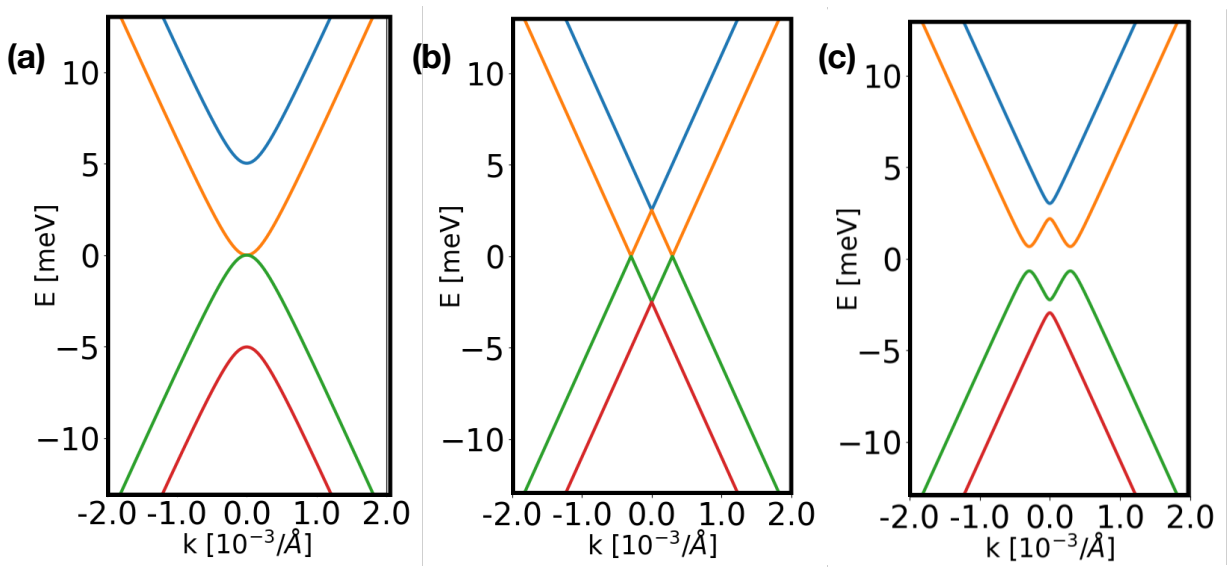

Figure S3: (a) Energy Dispersion with $\theta = \pi/2$ giving $\lambda_R = 2.51\ meV$ and $\lambda_{VZ} = 0\ meV$. (b) Energy Dispersion with $\theta = 0$ giving $\lambda_{VZ} = 2.51 meV$ and $\lambda_R = 0\ meV$. (c) The actual dispersion has possible values of $\lambda_{VZ} = 2.51\ \cos\theta$ meV and $\lambda_R = 2.51\ \sin\theta$ meV for any θ from 0 to 2π. We have chosen one such value from literature for λ_R giving $\theta = 13°$. This gives the dispersion as shown above with $\lambda_R = 0.56\ meV$ and $\lambda_{VZ} = 2.45\ meV$.

References

(1) Pizzocchero, F.; Gammelgaard, L.; Jessen, B. S.; Caridad, J. M.; Wang, L.; Hone, J.; Bøggild, P.; Booth, T. J. The hot pick-up technique for batch assembly of van der Waals heterostructures. Nature Communications **2016**, 7, 1–10.

(2) Wang, L.; Meric, I.; Huang, P.; Gao, Q.; Gao, Y.; Tran, H.; Taniguchi, T.; Watanabe, K.; Campos, L.; Muller, D.; Guo, J.; Kim, P.; Hone, J.; Shepard, K. L.; Dean, C. R. One-dimensional electrical contact to a two-dimensional material. Science **2013**, 342, 614–617.

(3) Smyth, C. M.; Addou, R.; McDonnell, S.; Hinkle, C. L.; Wallace, R. M. WSe2-contact metal interface chemistry and band alignment under high vacuum and ultra high vacuum deposition conditions. 2D Materials **2017**, 4, 025084.

(4) Wang, Y.; Yang, R. X.; Quhe, R.; Zhong, H.; Cong, L.; Ye, M.; Ni, Z.; Song, Z.; Yang, J.;

Shi, J., et al. Does p-type ohmic contact exist in WSe 2–metal interfaces? Nanoscale **2016**, 8, 1179–1191.

(5) Küppersbusch, C.; Fritz, L. Modifications of the Lifshitz-Kosevich formula in two-dimensional Dirac systems. Phys. Rev. B **2017**, 96, 205410.

(6) Lifshitz, I.; Kosevich, A. Theory of magnetic susceptibility in metals at low temperatures. Sov. Phys. JETP **1956**, 2, 636–645.

(7) Neto, A. C.; Guinea, F.; Peres, N. M.; Novoselov, K. S.; Geim, A. K. The electronic properties of graphene. Rev. Mod. Phys. **2009**, 81, 109.

(8) Novoselov, K. S.; Geim, A. K.; Morozov, S. V.; Jiang, D.; Katsnelson, M. I.; Grigorieva, I.; Dubonos, S.; Firsov, A. Two-dimensional gas of massless Dirac fermions in graphene. nature **2005**, 438, 197–200.